doi.org/10.36721/PJPS.2023.36.4.REG.1217-1225.1

Paeony attenuates high fat diet-induced kidney injury via inflammation inhibition

Qilu Fang[1,2], Qinglin Li[2], Like Zhong[1,2], Yajun Qi[1,2], Wenxiu Xin[1,2]* and Luo Fang[1,2]*

[1]Department of Pharmacy, The Cancer Hospital of the University of Chinese Academy of Sciences (Zhejiang Cancer Hospital), Zhejiang, China

[2]Institute of Basic Medicine and Cancer (IBMC), Chinese Academy of Sciences, Zhejiang, China

Abstract: High-fat diet (HFD) feeding is a risk factor for kidney damage with limited treatment options. This study explored the effect of total glucosides of paeony (TGP) for treating obesity-related kidney damage. C57BL/6 mice fed with HFD were used for *in vivo* experiments. Body weight, lipid and renal function indicators were measured. Hematoxylin and eosin, Masson, Sirius Red and F4/80 immunohistochemical staining were performed. Fibrosis levels, inflammatory factors, MyD88, IκB and p-Jun NH2-terminal kinase (JNK) were detected. SV40 cells were incubated with palmitic acid, transfected with siRNA MyD88 and/or treated with TGP. The expression of MyD88, IκB, p-JNK, fibrosis and inflammatory factors were detected. TGP considerably decreased HFD-induced body weight gain and serum lipid concentration but improved renal function. In addition, TGP inhibited renal fibrosis and inflammation and reduced MyD88 and p-JNK levels, whereas increased IκB levels. Moreover, silencing MyD88 decreased p-JNK levels while increasing IκB levels which may be the mechanism of TGP treatment. Our findings demonstrated that TGP treatment can ameliorate HFD-induced kidney injury via regulating JNK and IκB signals mediated by MyD88.

Keywords: Total glucosides of paeony, obesity-associated kidney damage, MyD88, inflammation, fibrosis.

INTRODUCTION

The incidence of obesity is increasing annually and at younger and younger ages. Alarmingly, 493 million people are estimated to be either obese or overweight by 2030 (Hruby and Hu, 2015). After accounting for traditional risk factors like diabetes, hyperlipidemia and hypertension, weight gain also directly increases the risk of obesity-related kidney damage (Lakkis and Weir, 2018; McPherson *et al*., 2019). High-fat diet (HFD) can cause glomerular structural and functional lesions, such as glomerular inflammation, nodular glomerulosclerosis, mesangial expansion and extracellular matrix deposition leading to kidney fibrosis (Kumar *et al*., 2021; Hall *et al*., 2019). Moreover, kidney damage caused by obesity is a substantial cause of end-stage renal disease (ERSD) (Ruiz-Ortega *et al*., 2020). The prevalence of obesity-induced kidney damage increased from 0.2% in 1986-1990 to 2.0% in 1996-2000 (Kambham *et al*., 2001). However, treatment options remain very limited due to controlling blood pressure and glycemic index (Wouk, 2021). Developing new therapeutic options is urgently needed to treat HFD-induced kidney injury.

The innate immune system and inflammatory response over activation may contribute to obesity-related kidney disease (Schetz *et al*., 2019). Since obesity is generally considered to be a systemic, low-grade inflammatory state (Gregor and Hotamisligil, 2011; Saltiel and Olefsky, 2017). Excess nutrition, especially fatty acids, directly damage the renal system. Saturated fatty acids can bind to toll-like receptors (TLRs), myeloid differentiation protein2 (MD2), or fetal bovine serum protein-A (FetA) to initiate inflammatory pathways, promote synthesis and release of chemokine and cause inflammation of the kidney (Jourde-Chiche *et al*., 2019; Wang *et al*., 2017). Consequently, HFD can increase the pro-inflammatory cytokines levels, including IL-1β, IL-6 and TNF-α and upregulates adhesion cytokines, leading to immune cells infiltration (Raftar *et al*., 2022; Duan *et al*., 2018). However, immuno-suppression attenuated nephropathy by reducing the renal inflammatory response (Zhu *et al*., 2017). Therefore, reducing inflammation may be a potential therapeutic direction for treating obesity-induced kidney damage.

Paeonia lactiflora Pall is a Chinese traditional herbal medicine. Total glycosides of paeony (TGP), extracted from *P. lactiflora* Pall roots, have been used for treating gynecological problems, cramps, pain and giddiness for over 1500 years in Chinese medicine (Tan *et al*., 2020; Wang *et al*., 2014b). TGP exhibited extensive activities of anti-inflammatory, anti-oxidative, anti-hepatic damage and immune-regulatory activities accompanied by low toxicity and fewer adverse effects (Tang *et al*., 2018). In 1998, the National Medical Products Administration approved TGP (Pafulin) to treat rheumatoid arthritis. Also, studies have shown that TGP can protect the kidneys against type 1 diabetes-induced damage (Shao *et al*., 2019). However, whether TGP could mitigate obesity-related kidney injury remains unclear. Therefore, this study aimed to examine the role of TGP on inflammation to cure obesity-induced kidney damage.

**Corresponding author:* e-mail: xinwx@zjcc.org.cn

MATERIALS AND METHODS

Materials

Total Glucosides of White Paeony Capsules purchased from Ningbo Lihua Pharmaceutical Co., Ltd. (PaFuLin, 300mg/tablet, H20055058) that was dissolution using 1% sodium carboxyl methyl cellulose (CMC-Na) in the animal experiment or DMSO in the cell experiments. PA was purchased from Sigma (St. Louis, MO). Anti-GAPDH, anti-IκB and anti-MyD88 were obtained from Santa Cruz (Santa Cruz, CA); and anti-p-JNK and anti-JNK were purchased from Cell Signaling (Danvers, MA). The immunohistochemistry kit (PV-9000) was purchased from Beyotime Biotechnology Inc. (China).

Cell culture

SV40 cells were purchased from the Institute of Biochemistry and Cell Biology (Shanghai, China) and grown in RPMI-1640 medium (Gibco, Eggenstein, Germany) containing 10% fetal bovine serum and 1% penicillin and streptomycin solution in an incubator with 95% air and 5% CO2 at 37°C.

Animals

Adult male C57BL/6 mice (18-22g) were purchased from the Animal Center of Academy of Sciences (Shanghai, China). The animals were kept in a stable environment (12:12 h light-dark cycle, 24°C temperature, 40%-60% humidity) and with free access to food and water. The animals were kept adaptively for at least 3 days before use. "The Detailed Rules and Regulations of Medical Animal Experiments Administration and Implementation" were followed (Document NO. 1998-55, Ministry of Public Health, P.R. China.).

Animal experiments

Four groups of twenty-eight male C57BL/6 mice were randomly selected: one group was fed with a regular diet and the remaining three groups were fed with HFD for 8 weeks. In the HFD group mice, vehicle dosing (1% CMC-Na solution) or orally TGP (100mg/kg and 200mg/kg per day, respectively) were administered (Pafulin, 300mg/ tablet, H20055058; Ningbo Lihua Pharmaceutical Co., Ltd, Ningbo, China) over 8 weeks. Body weight was recorded every 4 weeks. After 16 weeks, the mice were euthanized under ether anesthesia. Blood samples (300-500μL) were collected via the tail vein. Kidney tissues were collected from the left part of the kidney. Renal tissue samples were fixed overnight with 4% paraformaldehyde at 4°C to investigate pathology and quickly frozen in liquid nitrogen to analysis gene and protein.

Real-time quantitative PCR

Kidney tissues (50-100mg) was used for RNA extraction by TRIzol (Invitrogen, Carlsbad, CA, USA). cDNA was synthesized with 2-5μg of RNA using a two-step reverse transcription kit (TaKaRa, Tokyo, Japan). SYBR Green qPCR kit was used for real time quantitative PCR (TaKaRa, Tokyo, Japan) (Kuba *et al*., 2020). Levels of TNF-α, IL-6, IL-1β, collagen I, TGF-β, C-TGF and β-actin were quantified using the LightCycle® 480 II (Roche Diagnostic Canada, QC). The primer sequences are listed in table 1.

Histopathology

A single piece of kidney tissue from each mouse was fixed in 4% paraformaldehyde solution, embedded in paraffin, sliced and stained with H&E (Xue *et al*., 2021). Stained sections were viewed and photographed using a light microscope (400× amplification; Nikon, Tokyo, Japan).

Masson and Sirius red staining

Kidney sections of each group were prepared and stained for fibrosis analysis using the Masson trichrome staining kit and Sirius red solution (Beyotime Biotech, Nantong, China) (Xie *et al*., 2022). All stained sections were then viewed with a light microscope (200×amplification; Nikon, Tokyo, Japan).

F4/80 immunohistochemical stainning

Kidney tissues of each group were prepared, after deparaffinization and rehydration, pieces were dealt with 3% H_2O_2 for removing catalase and 5% bovine serum albumin to remove catalase and unspecific binding. The tissues were then incubated with primer antibody against mouse F4/80 (1:500) for 24 hours at 4°C. After washing, secondary antibody was used to incubate kidney tissues at room temperature for 1 h. And then the tissues were stained with 3,3′-diaminobenzidine and the nucleus with hematoxylin. The images were viewed and captured with an Olympus light microscope (400× amplification; Nikon, Tokyo, Japan) (Yang *et al*., 2020).

Western blot analysis

Western blotting was carried out according to the previously published methods. Collected cells or homogenized kidney tissue samples were lysed. Lysates (50-100μg) were separated by 10% sodium dodecyl-sulfate polyacrylamide gel electrophoresis and electro transferred on to a nitrocellulose membrane. Each membrane was pre-incubated for 1.5h at room temperature in Tris-buffered saline, pH 7.6, containing 0.05% Tween 20 and 5% non-fat milk. The membrane was then incubated with anti-MyD88, anti-pJNK, anti-IκB and anti-GAPDH antibodies. Overnight at 4°C, the membrane was incubated with secondary antibodies and visualized using enhanced chemiluminescence reagents (Bio-Rad, Hercules, CA) (Kuba *et al*., 2020).

Serum lipid and renal function index detection

Mice serum was collected and the serum lipid index including the TG, TCH and HDL, was detected. Furthermore, the renal function index including serum Cr,

blood BUN and albumin (ALB), was detected using commercial kits (Nanjing Jiancheng, Jiangsu, China) (Ding *et al*., 2018).

Ethical approval

Ethics approval (include appropriate approvals or waivers) All experiments with C57BL/6 mice were constructed in accordance with the Guidelines for the Care and Use of Laboratory Animals, which was presented by the National Institutes of Health and approved by the Ethics Committee of Zhejiang Cancer Hospital.

STATISTICAL ANALYSIS

Statistical differences were analyzed using analysis of variance and independent Students t-test using GraphPad Prism 5 statistic software (La Jolla, CA, USA). Data were expressed as the mean ± standard error of the mean (SEM). A difference of $p<0.05$ was considered statistically significant.

RESULTS

TGP decrease body weight and TG but increase HDL

Obese mice fed with HFD were treated with TGP (100 and 200mg/kg) or negative control. Body weight, TCH and TG increased markedly in the HFD-fed group compared to those in the control group (table 2). Furthermore, with TGP treatment, there were considerable decrease in body weight and TG levels. However, HFD-fed and TGP-treated groups did not show significant difference in TCH levels. Moreover, significantly elevated HDL levels were noted. These results suggest that TGP protect mice from obesity-induced hyperlipidemia.

TGP prevent kidneys damage

Next, we detected serum Cr, BUN and ALB. HFD-fed mice with kidney disease exhibited elevated levels of Cr, BUN and ALB, which were drastically conversed by TGP at a dose of 200mg/kg (figs. 1A-1C). Furthermore, we conducted H&E staining to investigate renal tubules and glomeruli changes. Compared to the control group, the kidney tissue morphology in HFD-fed mice was considerably different, with tubular epithelial cell shedding and vacuolar degeneration, glomerular shrinkage and glomerular basement membrane thickening (fig. 1D). However, when treated with TGP, the lesions improved. These results suggest that TGP protects mice from obesity-induced kidney lesions.

TGP reduced kidney fibrosis

Then, we evaluated the fibrosis in the kidneys. Sirius Red and Masson staining for collagen both revealed fibrotic lesions in the kidneys of HFD-fed mice (figs. 2A and 2B). The mRNA levels of collagen I, TGF-β and C-TGF significant increased in HFD-fed mice compared to those in the control group. However, TGP distinctly conversed this increase (figs. 2C-2E). These results suggest that TGP protects mice from obesity-associated kidney fibrosis.

TGP reduce kidney inflammation

Inflammation is an essential pathological process leading to kidney damage caused by obesity. Therefore, we examined whether TGP could inhibit HFD-induced kidney inflammation. F4/80 immunohistochemical staining showed that HFD-fed had increased F4/80 levels, indicating high macrophage infiltration, which was significantly decreased with TGP treatment (fig. 3A). Furthermore, we investigated pro-inflammatory cytokines mRNA levels, including TNF-α (fig. 3B), IL-6 (fig. 3C), IL-1β (fig. 3D). TGP treatment reversed the HFD-induced the increase in pro-inflammatory cytokines. These results suggest that TGP protects mice from obesity-induced kidney inflammation.

TGP inhibited hyperlipidemia-induced activation of NF-κB and p-JNK signals via MyD88

To explore whether TGP's anti-inflammatory effect was mediated by MyD88 inhibition mediating NF-κB and JNK, the MyD88, phosphorylated JNK and IκB levels were determined. MyD88 and phosphorylated JNK levels were markedly increased in the HFD-fed group. However, these levels were reduced by TGP treatment. HFD also induced IκB degradation, however, TGP treatment reversed this degradation (fig. 4A). Palmitic acid (PA) is the most abundant and widespread FFA and is commonly used as a representative FFA to stimulate cellular stress response. Therefore, we used PA (200μM) as a stimulant to investigate the effect of TGP. As expected, PA induced an increase in MyD88 and phosphorylated JNK, however, TGP (150μg/ml or 300μg/ml) reversed the decrease in IκB (fig. 4B). We further silenced MyD88 and detected phosphorylated JNK and IκB levels. Silencing MyD88 suppressed PA-induced activation of NF-κB and JNK by decreasing the JNK phosphorylation and degradation IκB (fig. 4C). These results suggest that TGP inhibited hyperlipidemia -induced inflammation via MyD88 mediating NF-κB and JNK.

TGP reduce the fibrosis and inflammatory factors in PA-stimulated SV40 cells

SV40 cells were first pre-treated with PA alone (200μM) or combined with TGP (150μg/ml or 300μg/ml). PA induced an increased in fibrosis cytokines TGF-β, collagen I and C-TGF in SV40 cells, while TGP dose-dependently reduced those cytokines (fig. 5A-C). Moreover, TGP also inhibited the mRNA expression of inflammatory markers, such as TNF-α, IL-6 and IL-1β in a dose-dependent manner (figs. 5D-5F). These results suggest that TGP inhibited PA-induced fibrosis and inflammation in SV40 cells.

Table 1: Primer sequences.

Gene	Primer sequences
TGF-β	Forward primer: GGACACTGGTACATAGCTCAAGT Reverse primer: TGCATAGCAGATGGATTCATTCC
Collagen1	Forward primer: AGATGGCTGTAATGGAACTCAAG Reverse primer: CCAGGTGGTCCTAAAATCCCAG
Collagen4	Forward primer: GACCCAACTATGATGCGAGCC Reverse primer: CCCATCCCACAGGTCTTAGAAC
TNF-α	Forward primer: GTGGAAGCATTGTGCTCAAATC Reverse primer: CCCCGTTGCAGGGTTGTAAT
IL-6	Forward primer: GGCGGATCGGATGTTGTGAT Reverse primer: GGACCCCAGACAATCGGTTG
IL-1β	Forward primer: TGCCACCTTTTGACAGTGATG Reverse primer: AAGGTCCACGGGAAAGACAC
β-actin	Forward primer: CGTCATTGCACGAAGACACAA Reverse primer: CCTGGTCCACCATTTTAAGGC

Table 2: TGP slowed body weight gain in HFD-mice (n=7).

Groups	First month(g)	Second month(g)	Third month(g)	Fourth month(g)
Control	20.1±0.6	23.4±0.2	25.4±0.1	27.9±0.6
HFD	21.2+0.8	28.1±0.6	$37.4\pm0.8^{\#\#}$	$50.1\pm0.5^{\#\#\#}$
HFD+TGP-100mg/kg	20.3±0.2	25.9±0.2	32.4±0.5	$39.8\pm0.7^{*}$
HFD+TGP-200mg/kg	21.8±0.3	25.4±0.3	$30.4\pm0.4^{*}$	$36.8\pm0.2^{**}$

$^{\#\#}p<0.01$, $^{\#\#\#}p<0.001$, HFD group vs Control group; $^{*}p<0.05$, $^{**}p<0.01$, TGP group vs HFD group

Table 3: TGP improved hyperlipidemia in HFD-mice (n=7).

Groups	TCH (mg/dl)	TG (mg/dl)	HDL (mg/dl)
Control	278.1±0.6	59.5±0.9	117.8±0.4
HFD	$728.9\pm0.8^{\#\#\#}$	$100.9\pm0.8^{\#\#}$	$74.4\pm0.3^{\#\#}$
HFD+TGP-100mg/kg	708.3±0.2	80.5±0.7	86.1±0.4
HFD+TGP-200mg/kg	664.8±0.3	$67.8\pm0.6^{*}$	$102.3\pm0.2^{*}$

$^{\#\#}p<0.01$, $^{\#\#\#}p<0.001$, HFD group vs Control group; $^{*}p<0.05$, TGP group vs HFD group

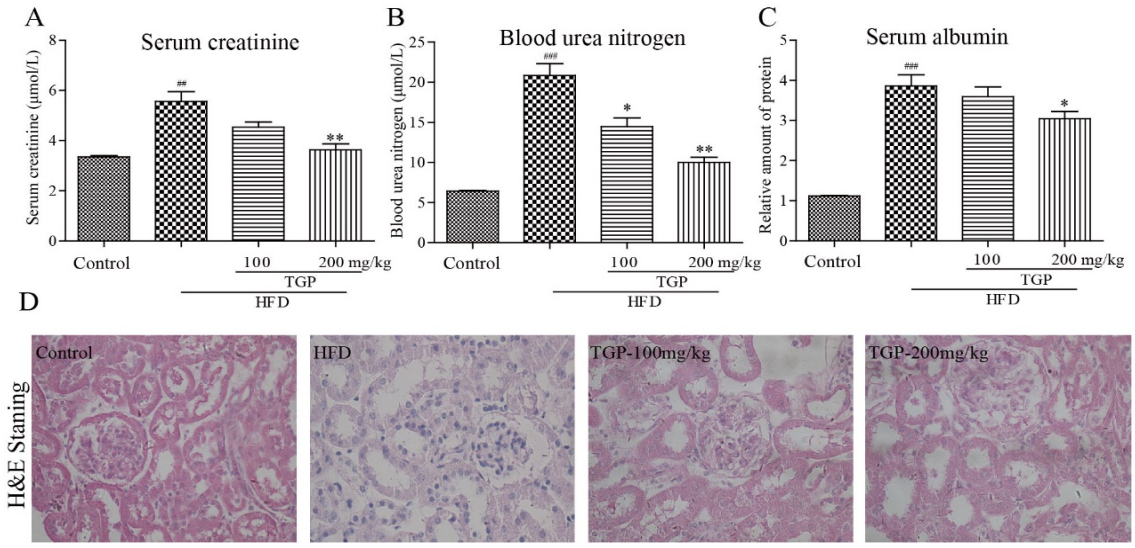

Fig. 1: TGP improved the pathology and histology of HFD mice. Mice serum was collected and analyzed. TGP treatment reduced the increased serum Cr (A), BUN (B) and ALB levels (C) in HFD-fed mice. (D) TGP treatment improved kidney histological abnormalities in HFD-fed mice (400×magnification). . Histological analysis using H&E staining showed that TGP treatment significantly improved glomerular shrinking and tubular necrosis. Data are presented as the means ± SEM (n=7 in each group; HFD group vs Control group, $^{\#\#\#}p<0.001$, $^{\#\#}p<0.01$; TGP group vs HFD group, $^{*}p<0.05$, $^{**}p<0.01$) ALB: albumin; BUN: blood urea nitrogen; Cr: creatinine; HFD: high-fat diet; TGP: total glucosides of paeony.

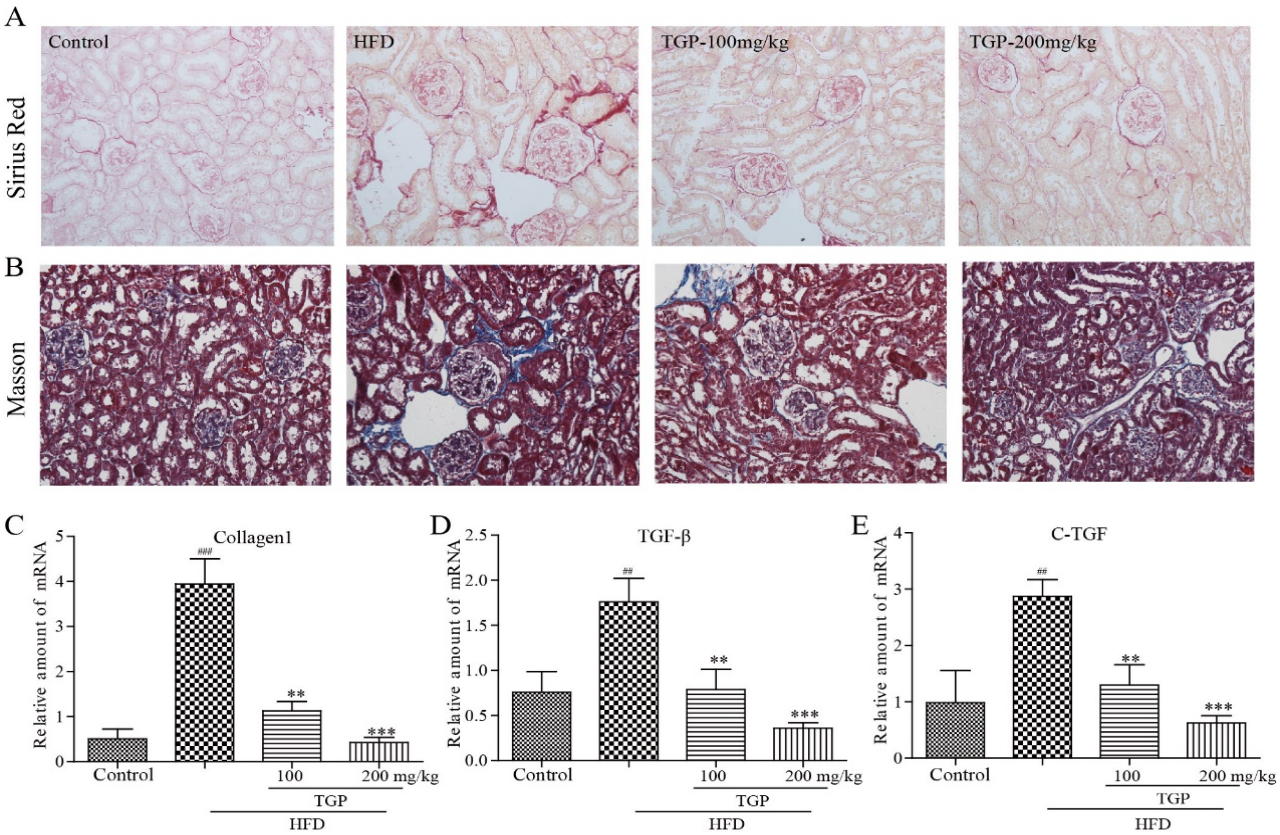

Fig. 2: TGP inhibited kidney fibrosis in HFD mice. (A-B) TGP treatment considerably decreased kidney fibrosis in HFD-fed mice, as indicated by Sirius Red staining (red) and Masson staining (blue) (200×magnification). (C-E) TGP treatment significantly inhibited the expression of fibrosis markers including collagen I (C), TGF-β (D) and C-TGF (E) at the increased level in HFD-fed mice. Data are means ± SEM (n=7 in each group; HFD group vs Control group, $^{###}p<0.001$, $^{##}p<0.01$; TGP group vs HFD group, $^{**}p<0.01$, $^{***}p<0.001$). HFD: high-fat diet; TGP: total glucosides of paeony.

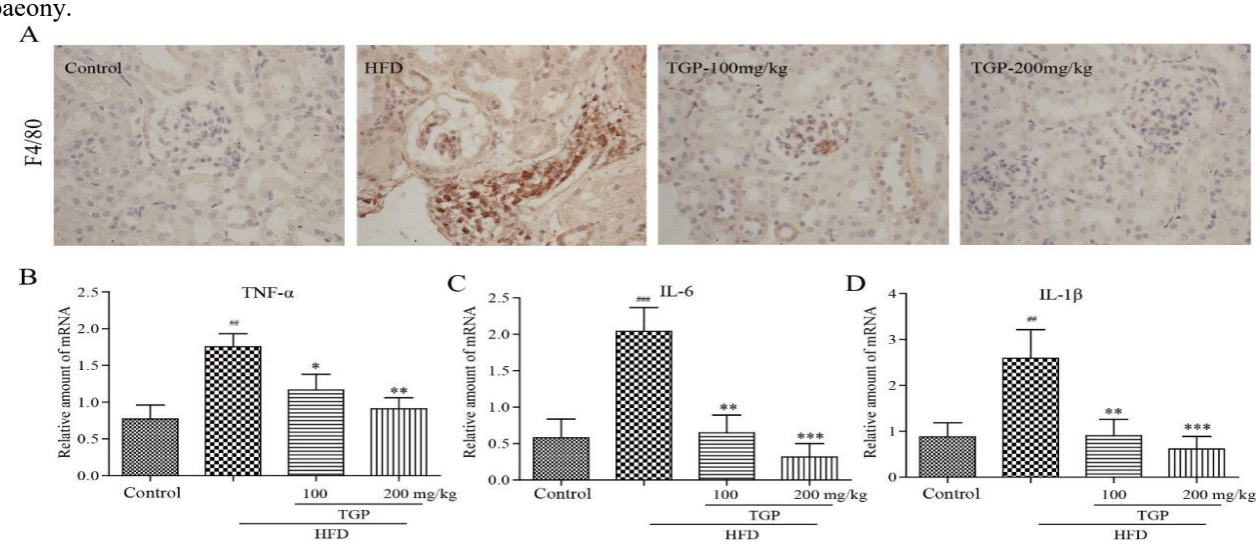

Fig. 3: TGP inhibited kidney inflammatory responses in HFD mice. Kidney tissues in each group were collected and analyzed. (A) TGP treatment inhibited kidney macrophage infiltration in HFD-fed mice. F4/80 staining was used to detected macrophage infiltration (400×magnification). (B-D) TGP treatment reduced kidney inflammatory genes expression, including TNF-α (B), IL-6 (C) and IL-1β (D) in HFD-fed mice. Data are presented as the means ± SEM (n=7 in each group; HFD group vs Control group, $^{###}p<0.001$, $^{##}p<0.01$; TGP group vs HFD group, $^{*}p<0.05$, $^{**}p<0.01$, $^{***}p<0.001$). HFD: high-fat diet; TGP: total glucosides of paeony.

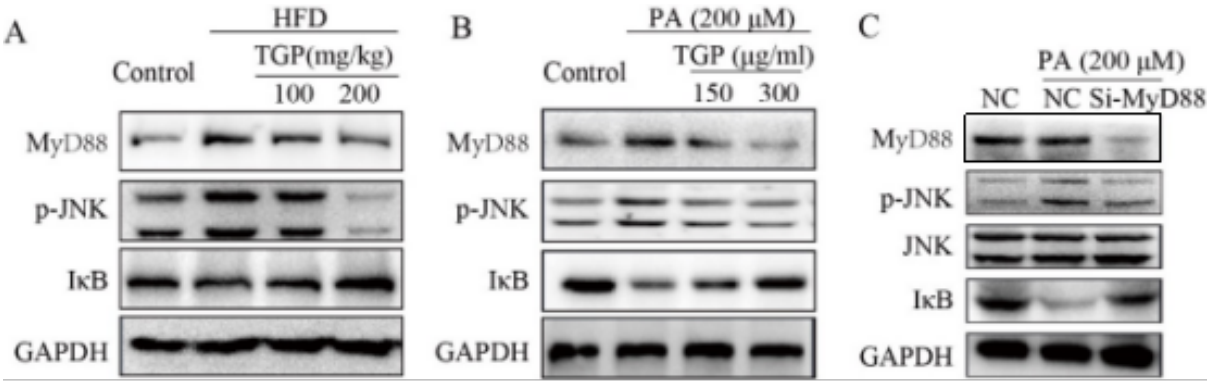

Fig. 4: TGP inactivated MyD88-mediating JNK and IκB in hyperlipemia. Kidney tissues in each group were collected and analyzed. (A) TGP treatment inhibited MyD88 expression and JNK and IκB activation using western blotting in HFD-fed mice. (B) TGP treatment inhibited MyD88 expression and JNK and IκB activation using western blotting in PA-stimulated SV40 cells. (C) Silencing MyD88 in SV40 cells inhibited activation of JNK and IκB using western blotting. Data are expressed as the means ± SEM. PA: palmitic acid; TGP: total glucosides of paeony.

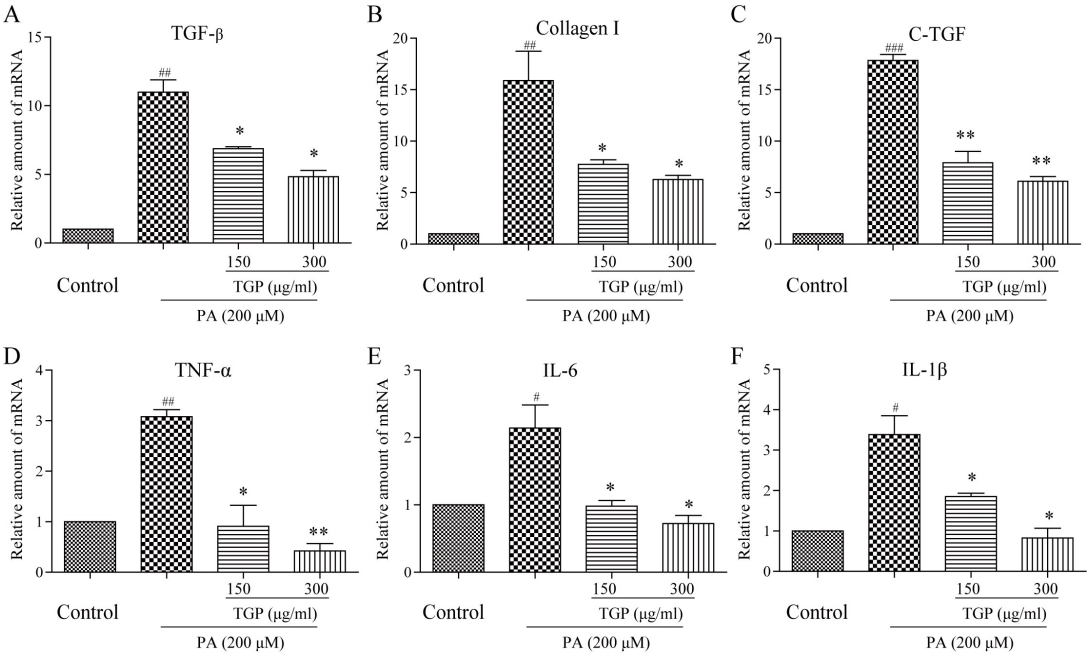

Fig. 5: TGP inhibited fibrosis and inflammatory cytokines secretion in PA-stimulated SV40 cells. SV40 cells were pre-treated with TGP (150 or 300μg/ml) or with a vehicle (DMSO, 3μL) for 1 h before stimulation with PA (200μM) for 48h. (A-C) TGP significantly inhibited PA-induced expression of fibrosis genes, including TGF-β (A), collagen I (B) and C-TGF (C) using RT-qPCR analysis of PA-stimulated SV40 cells. (D-F) TGP significantly inhibited PA-induced expression of inflammatory genes expression, including TNF-α (D), IL-6 (E) and IL-1β (F) detected by RT-qPCR analysis of PA-stimulated SV40 cells. Data are expressed as the means ± SEM ((PA group vs Control group, $^{\#}p<0.05$, $^{\#\#}p<0.01$, $^{\#\#\#}p<0.001$; TGP group vs PA group, $^{*}p<0.05$, $^{**}p<0.01$). PA: palmitic acid; TGP: total glucosides of paeony.

DISCUSSION

Obesity is a substantial risk factor for chronic kidney disease. Furthermore, obesity can lead to structural and histopathological changes in the kidneys by affecting renal hemodynamics, angiotensin-aldosterone system and insulin resistance thus causing nephropathy (Hall *et al*., 2021; Hall *et al*., 2019). However, the treatment options are still limited, resulting in an increased incidence of end-stage renal disease. Therefore, new methods or drugs are urgently needed to treat obesity-induced kidney damage. Traditional Chinese herbal extracts or monomers can effectively delay the progression of obesity-related kidney disease and have a strong potential market in treating chronic diseases. Consequently, we explored TGP to protect the kidneys against obesity-induced renal injury. To the best of our knowledge, this is the first study to investigate the therapeutic effect of TGP on obesity-related kidney disease.

TGP is recognized as a valuable traditional herb to treat rheumatoid arthritis, systemic lupus erythematosus and hepatitis.

Moreover, TGP reportedly cured, Heymann nephritis, IgA nephropathy and diabetic nephropathy. Additionally, TGP extracted from *Radix Paeoniae Alba* can reduce blood lipids and enhance insulin sensitivity (Chang *et al*., 2021; Chen *et al*., 2020). In this study, C57BL/6 mice fed with HFD showed obesity, elevated serum Cr, BUN, urea ALB levels and pathological changes, including glomerular enlargement and thickened glomerular basement membranes, renal fibrosis and collagen accumulation. However, TGP administration ameliorated obesity-induced kidney pathology and histological changes, decreasing Cr, BUN and ALB levels. We also observed an inhibiting effect of TGP on inflammation by reducing macrophage infiltration and inflammatory factors release in HFD-fed mice's kidneys.

Increased cytokine production and inflammatory cell infiltration in tissues promotes the progression of obesity-related kidney damage (Gregor and Hotamisligil, 2011; Manabe, 2011). Inflammation is the early pathology of renal disease, which can promote kidney fibrosis and sclerosis, resulting in renal function disruption, which leads to end-stage renal disease (Arabi *et al*., 2022; Stone *et al*., 2017). Macrophage infiltration in kidneys is associated with increased inflammatory level leading to kidney damage. However, reducing the pro-inflammatory macrophages infiltration in kidneys successfully improved renal damage (Kavvadas *et al*., 2018). Macrophages infiltrating to renal tissue secrete inflammatory factors to stimulate inflammatory kidney lesions and cause apoptosis to induce the kidney necrosis (Liang *et al*., 2021; Palau *et al*., 2021). Therefore, anti-inflammatory treatment by inhibiting the inflammatory response in kidneys may be the prevention or treatment of obesity-induced kidney damage.

TGP could inhibit the progression of inflammation-related diseases, such as autoimmune diseases, enteritis and hepatitis, diabetes and had an inhibitory effect on fibrosis and apoptosis caused by inflammation (Jin and Zhang, 2022; Zhang *et al*., 2022). In addition, TGP was also effective in inducing the production of M2-type anti-inflammatory macrophages production (Jin *et al*., 2022). In this study, the increase of phosphorylated JNK and degradation of IκB in HFD-fed mice and PA-stimulated SV40 cells could be reversed by TGP. These results support the ability of TGP to protect against hyperlipidemia-induced renal damage.

Transcription factor nuclear activation of factor-kappa B (NF-κB) plays a central role in regulating inflammation by regulating pro-inflammatory cytokines, chemokines and cell adhesion molecules (Yu *et al*., 2020). Once activated, IκB is phosphorylated and degraded, resulting in its subunit, p65, migrating into the nucleus to activate the expression of its downstream genes expression. Moreover, JNK is another responsive kinase to obesity which represents a possible target for therapeutic intervention in obese patients. Studies demonstrate that JNK is required to establish obesity-induced insulin resistance and inflammation (Solinas and Becattini, 2017). MyD88 is the common upstream gene of NF-κB and JNK signals. MyD88 is a typical adapter of inflammatory signaling pathways for the toll-like receptor (TLR) and interleukin-1 (IL-1) receptors, leading to various functional outputs, including NF-κB, mitogen-activated protein kinases (MAPK) and signal transducer and activators of transcription 3 (STAT3). *In vivo* and *in vitro*, we all found that TGP inhibited MyD88 expression and silencing MyD88 in SV40 cells inhibited the activation of the NF-κB and JNK pathways activation. These results support the hypothesis that MyD88 mediated the anti-inflammatory effect of TGP and maybe a target of obesity-related kidney damage.

CONCLUSION

The results of this study indicate that TGP is an effective therapeutic agent for treating obesity-induced kidney damage. TGP treatment inhibited inflammation by blocking inflammatory cytokines release and immune cell infiltration and exhibited substantial improvements in histological abnormalities and fibrosis. The results showed that TGP could reduce the expression of MyD88 and inhibit IκB degradation and JNK phosphorylation and the TGP mechanism may be inhibiting MyD88-mediating JNK and IκB.

ACKNOWLEDGEMENTS

We would like to give our thanks to Prof. Luo Fang for valuable discussion. This research was funded by the Medical Health Science and Technology Project of Zhejiang Province (No. 2022KY105 and 2017190933), National Natural Science Foundation of Zhejiang Province (No. LY22H280015, YY19H310003 and LYY18H310006) and National Natural Science Foundation of China (No. 81903898 and 81803585).

REFERENCES

Arabi T, Shafqat A, Sabbah BN, Fawzy NA, Shah H, Abdulkader H, Razak A, Sabbah AN and Arabi Z (2022). Obesity-related kidney disease: Beyond hypertension and insulin-resistance. *Front. Endocrinol. (Lausanne)*, **13**: 1095211.

Bayer AL and Alcaide P (2021). MyD88: At the heart of inflammatory signaling and cardiovascular disease. *J. Mol. Cell Cardiol*., **161**: 75-85.

Chang X, Zhang P, Xu XX and Pang B (2021). Total

glucosides of paeony inhibited autophagy and improved acute kidney injury induced by ischemia-reperfusion via the lncRNA TUG1/miR-29a/PTEN Axis. *Drug Des. Devel. Ther.,* **15**: 2229-2242.

Chen F, Hu Y, Xie Y, Zhao Z, Ma L, Li Z and Tan W (2020). Total glucosides of paeony alleviate cell apoptosis and inflammation by targeting the long noncoding RNA XIST/MicroRNA-124-3p/ITGB1 axis in renal ischemia/reperfusion injury. *Mediators Inflamm.,* **2020**: 8869511.

Ding T, Wang S, Zhang X, Zai W, Fan J, Chen W, Bian Q, Luan J, Shen Y, Zhang Y, Ju D and Mei X (2018). Kidney protection effects of dihydroquercetin on diabetic nephropathy through suppressing ROS and NLRP3 inflammasome. *Phytomedicine,* **41**: 45-53.

Gregor MF and Hotamisligil GS (2011). Inflammatory mechanisms in obesity. *Annu. Rev. Immunol.,* **29**: 415-445.

Hall JE, Mouton AJ, da Silva AA, Omoto ACM, Wang Z, Li X and do Carmo JM (2021). Obesity, kidney dysfunction and inflammation: Interactions in hypertension. *Cardiovasc. Res.,* **117**(8): 1859-1876.

Hruby A and Hu FB (2015). The Epidemiology of obesity: A big picture. *Pharmacoeconomics,* **33**(7): 673-689.

Jin L, Guo Y, Mao W, Wang J, Jin L, Liu X, Shou Q and Fu H (2022). Total glucosides of paeony inhibit breast cancer growth by inhibiting TAMs infiltration through NF-κB/CCL2 signaling. *Phytomedicine,* **104**: 154307.

Jin Y and Zhang A (2022). Total glucosides of paeony ameliorates oxidative stress, apoptosis and inflammatory response by regulating the Smad7 TGF β pathway in allergic rhinitis. *Mol. Med. Rep.,* **25**(3): 83.

Jourde-Chiche N, Fakhouri F, Dou L, Bellien J, Burtey S, Frimat M, Jarrot PA, Kaplanski G, Le Quintrec M, Pernin V, Rigothier C, Sallée M, Fremeaux-Bacchi V, Guerrot D and Roumenina LT (2019). Endothelium structure and function in kidney health and disease. *Nat. Rev. Nephrol.,* **15**(2): 87-108.

Kambham N, Markowitz GS, Valeri AM, Lin J and D'Agati VD (2001). Obesity-related glomerulopathy: An emerging epidemic. *Kidney Int.,* **59**(4): 1498-1509.

Kavvadas P, Keuylian Z, Prakoura N, Placier S, Dorison A, Chadjichristos CE, Dussaule JC and Chatziantoniou C (2018). Notch3 orchestrates epithelial and inflammatory responses to promote acute kidney injury. *Kidney Int.,* **94**(1): 126-138.

Kuba Y, Kyan H, Iha Y, Kato T, Oyama M, Miyahira M, Kakita T, Takara T, Yamauchi M, Kamiya H, Sunagawa T, Kawakami Y, Nidaira M, Kudaka J, Yamakawa M, Itokazu T and Itokazu K (2020). Emergent measles-containing vaccination recommendation for aged 6-11 months and detection of vaccine-associated measles during a large measles outbreak in Okinawa, Japan, in 2018. *Vaccine,* **38**(10): 2361-2367.

Kumar A, Sundaram K, Mu J, Dryden GW, Sriwastva MK, Lei C, Zhang L, Qiu X, Xu F, Yan J, Zhang X, Park JW, Merchant ML, Bohler HCL, Wang B, Zhang S, Qin C, Xu Z, Han X, McClain CJ, Teng Y and Zhang HG (2021). High-fat diet-induced upregulation of exosomal phosphatidylcholine contributes to insulin resistance. *Nat. Commun.,* **12**(1): 213.

Lakkis JI and Weir MR (2018). Obesity and kidney disease. *Prog Cardiovasc Dis,* **61**(2): 157-167.

Liang CL, Jiang H, Feng W, Liu H, Han L, Chen Y, Zhang Q, Zheng F, Lu CJ and Dai Z (2021). Total glucosides of paeony ameliorate pristane-induced lupus nephritis by inducing PD-1 ligands(+) macrophages via activating IL-4/STAT6/PD-L2 signaling. *Front Immunol.,* **12**: 683249.

Manabe I (2011). Chronic inflammation links cardiovascular, metabolic and renal diseases. *Circ. J.,* **75**(12): 2739-2748.

McPherson KC, Shields CA, Poudel B, Fizer B, Pennington A, Szabo-Johnson A, Thompson WL, Cornelius DC and Williams JM (2019). Impact of obesity as an independent risk factor for the development of renal injury: Implications from rat models of obesity. *Am. J. Physiol. Renal Physiol.,* **316**(2): F316-f327.

Palau V, Jarrín J, Villanueva S, Benito D, Márquez E, Rodríguez E, Soler MJ, Oliveras A, Gimeno J, Sans L, Crespo M, Pascual J, Barrios C and Riera M (2021). Endothelial ADAM17 expression in the progression of kidney injury in an obese mouse model of pre-diabetes. *Int. J. Mol. Sci.,* **23**(1): 221.

Raftar SKA, Ashrafian F, Abdollahiyan S, Yadegar A, Moradi HR, Masoumi M, Vaziri F, Moshiri A, Siadat SD and Zali MR (2022). The anti-inflammatory effects of Akkermansia muciniphila and its derivates in HFD/CCL4-induced murine model of liver injury. *Sci. Rep.,* **12**(1): 2453.

Ruiz-Ortega M, Rayego-Mateos S, Lamas S, Ortiz A and Rodrigues-Diez RR (2020). Targeting the progression of chronic kidney disease. *Nat. Rev. Nephrol.,* **16**(5): 269-288.

Saltiel AR and Olefsky JM (2017). Inflammatory mechanisms linking obesity and metabolic disease. *J. Clin. Invest.,* **127**(1): 1-4.

Schetz M, De Jong A, Deane AM, Druml W, Hemelaar P, Pelosi P, Pickkers P, Reintam-Blaser A, Roberts J, Sakr Y and Jaber S (2019). Obesity in the critically ill: A narrative review. *Intensive Care Med.,* **45**(6): 757-769.

Shao YX, Gong Q, Qi XM, Wang K and Wu YG (2019). Paeoniflorin ameliorates macrophage infiltration and activation by inhibiting the TLR4 signaling pathway in diabetic nephropathy. *Front Pharmacol.,* **10**: 566.

Solinas G and Becattini B (2017). JNK at the crossroad of obesity, insulin resistance and cell stress response. *Mol. Metab.,* **6**(2): 174-184.

Tan YQ, Chen HW, Li J and Wu QJ (2020). Efficacy, chemical constituents and pharmacological actions of radix paeoniae rubra and radix paeoniae alba. *Front Pharmacol.,* **11**(2): 1054.

Wouk N (2021). End-Stage renal disease: Medical management. *Am. Fam. Physician,* **104**(5): 493-499.

Xie J, Ye Z, Li L, Xia Y, Yuan R, Ruan Y and Zhou X (2022). Ferrostatin 1 alleviates oxalate induced renal tubular epithelial cell injury, fibrosis and calcium oxalate stone formation by inhibiting ferroptosis. *Mol. Med. Rep.,* **26**(2): 256.

Xue M, Yang F, Le Y, Yang Y, Wang B, Jia Y, Zheng Z and Xue Y (2021). Klotho protects against diabetic kidney disease via AMPK- and ERK-mediated autophagy. *Acta Diabetol.,* **58**(10): 1413-1423.

Yang L, Guo J, Yu N, Liu Y, Song H, Niu J and Gu Y (2020). Tocilizumab mimotope alleviates kidney injury and fibrosis by inhibiting IL-6 signaling and ferroptosis in UUO model. *Life Sci.,* **261**: 118487.

Yu H, Lin L, Zhang Z, Zhang H and Hu H (2020). Targeting NF-κB pathway for the therapy of diseases: Mechanism and clinical study. *Signal Transduct. Target Ther.,* **5**(1): 209.

Zhang J, Fu Y, Yang B and Xiang X (2022). Total glucosides of paeony inhibits liver fibrosis and inflammatory response associated with cirrhosis via the FLI1/NLRP3 axis. *Am. J. Transl. Res.,* **14**(6): 4321-4336.

Zhu P, Sieben CJ, Xu X, Harris PC and Lin X (2017). Autophagy activators suppress cystogenesis in an autosomal dominant polycystic kidney disease model. *Hum. Mol. Genet.,* **26**(1): 158-172.